Electronic Supplementary information

High water permeance and ions rejection through F-graphene oxide membrane

Wuerkaixi Maimuli[1#], Rujie Yang[2#], Shuai Wang[2], Junfan Liu[1], Fangfang Dai[3,4], Jun Wang[2], Lu Li[5], Liang Chen[6,1]* and Shanshan Liang[2]*

[1]Department of Environment and Resources, Zhejiang A&F University, Hangzhou 311300, China
[2]School of Physics, East China University of Science and Technology, Shanghai, 200237, China
[3]Wenzhou Institute, University of Chinese Academy of Sciences, Wenzhou, 325000, China
[4]Oujiang Laboratory (Zhejiang Lab for Regenerative Medicine, Vision and Brain Health), Wenzhou, 325001, China
[5]College of Chemistry and Materials Engineering, Zhejiang A&F University, Hangzhou 311300, China
[6]School of Physical Science and Technology, Ningbo University, Ningbo 315211, China

Corresponding Email: liangshanshan@ecust.edu.cn and chenliang2@nbu.edu.cn
[#] *These authors contributed equally to this work.*

Contents

PS 1 AFM results of pristine GO nanosheets

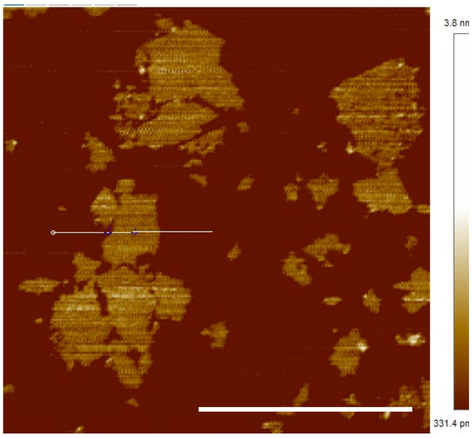

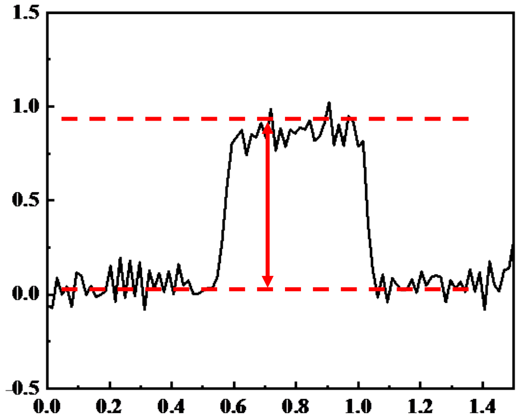

Fig. S1 (a) AFM image of pristine GO nanosheets. (b) The corresponding height profile of pieces from(a).

PS2. The molecule structure of 2,4-diamino-6-(4-fluorophenyl) pyrimidine.

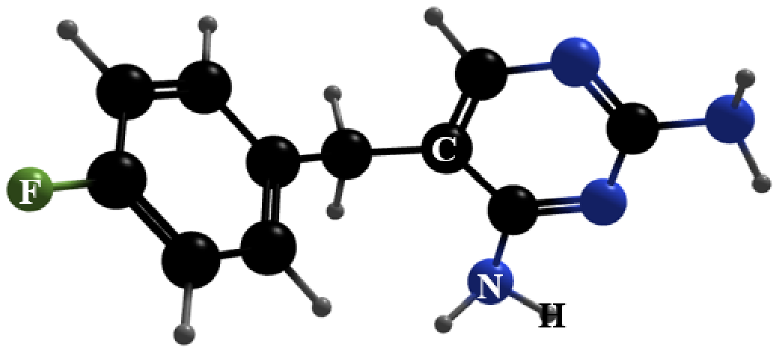

Fig. S2 The molecule structure of 2,4-diamino-6-(4-fluorophenyl) pyrimidine.

PS3. Property of GO-based suspensions

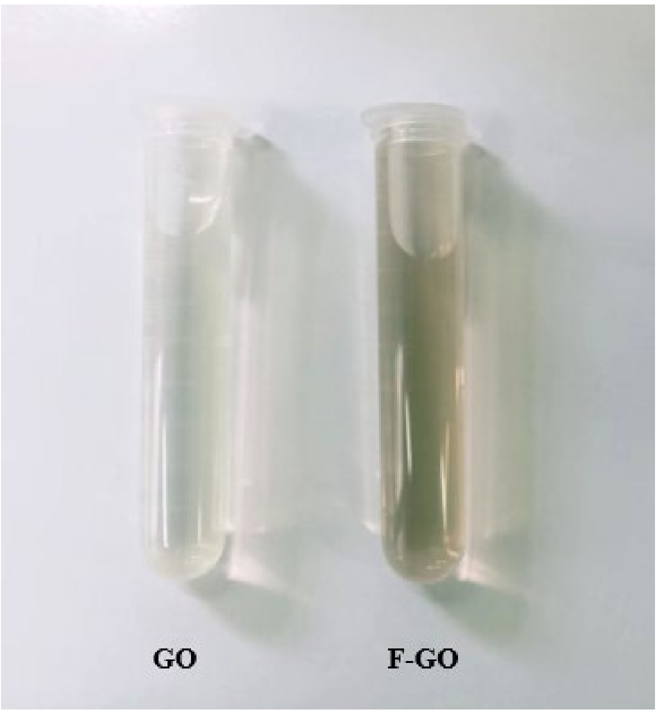

Fig. S3. Optical photo of GO and F-GO suspensions.

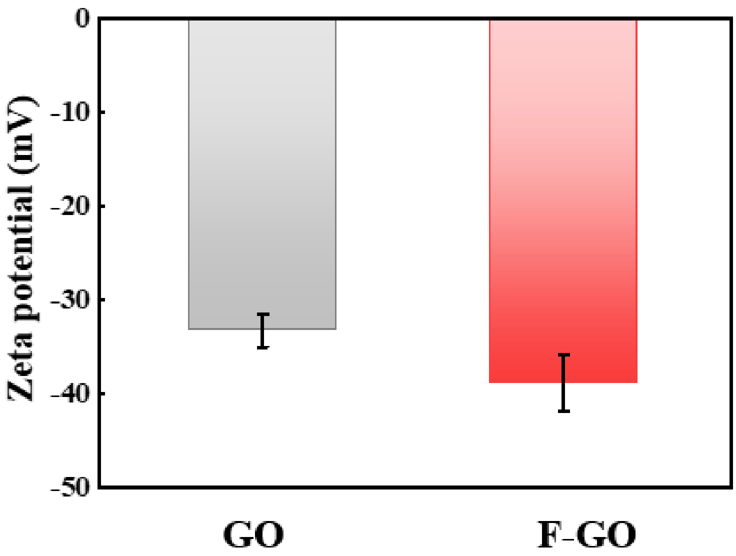

Fig. S4 Zeta potential of GO and F-GO suspensions.

PS4 SEM image of F-GO membrane.

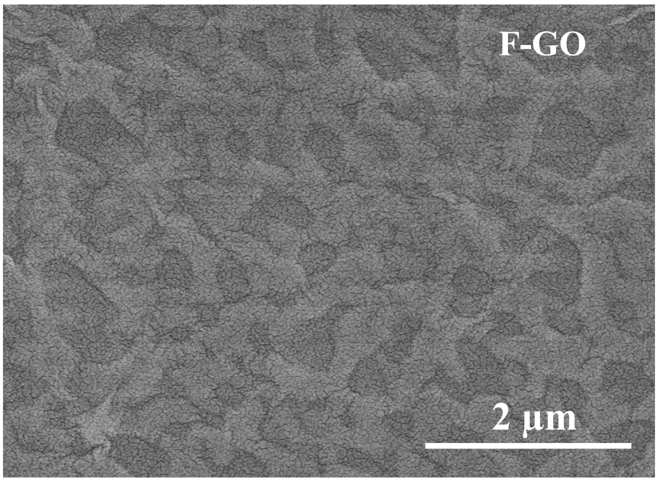

Fig. S5 SEM surface image of F-GO membrane.

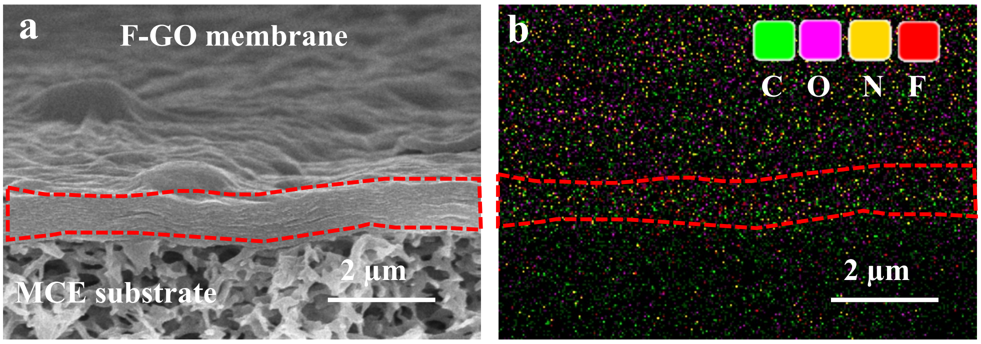

Fig. S6 (a) SEM/EDX images of cross-section of the F-GO membrane, where the enclosed image is mapped for the distribution of atoms; (b) EDX mapping of carbon atoms, oxygen atoms, nitrogen atoms, fluorine atoms on the cross-section of the F-GO membrane.

PS5. XPS spectra of the GO and F-GO membranes

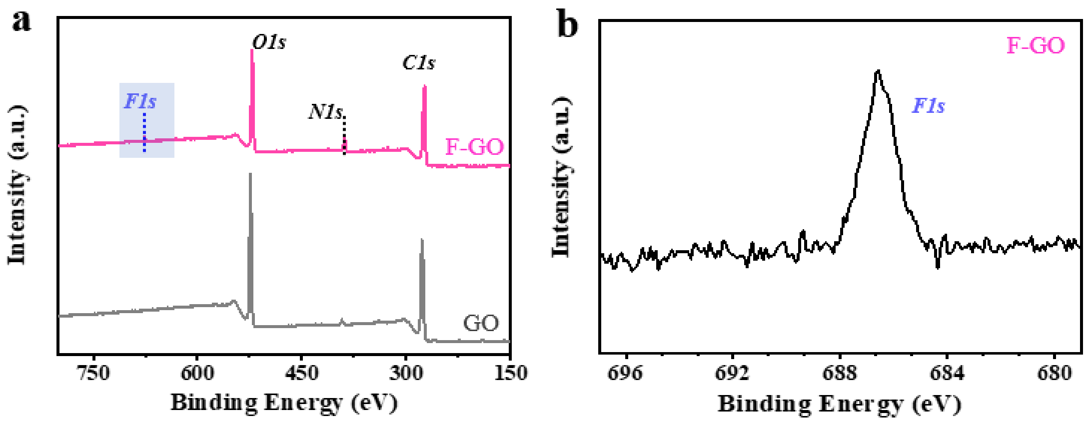

Fig. S7 (a) XPS wide scan of the prepared GO and F-GO membranes. (b)XPS spectra of the GO and F-GO membranes for F1s core level.

Table S1 Element composition of GO and F-GO membrane.

Membranes	Element composition				
	C (at.%)	O (at.%)	N (at.%)	F (at.%)	C/O
GO	67.67	32.33	-	-	2.09
F-GO	66.86	25.80	6.47	0.87	2.59

Table S2 XPS Element composition with different etch depth of F-GO membrane.

Etch depth (nm)	Element composition			
	C (at.%)	O (at.%)	N (at.%)	F (at.%)
0	66.8	25.27	6.25	1.58
10	84.81	7.19	6.21	1.7
20	85.92	6.83	5.67	1.58
30	85.49	6.83	5.97	1.71

PS6. FT-IR spectra of the GO and F-GO membranes.

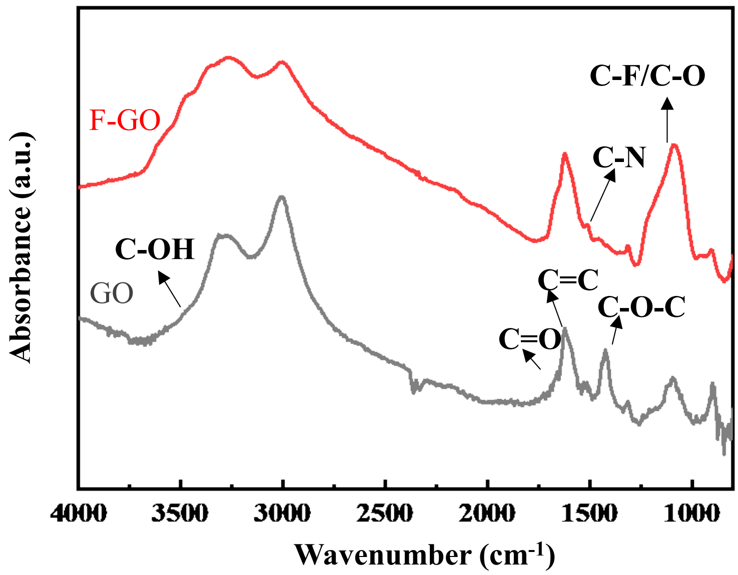

Fig. S8 FT-IR spectra of the GO and F-GO membranes.

PS7. Ion adsorption performances of the F-GO membranes.

After F-GO membranes were prepared using vacuum filtration, 300 mL 50 mg L^{-1} $FeCl_3$ solutions were added to the feed side. The salt solution was stirred with a blender at ~180 rpm without filtration. Afterwards, the samples solutions were collected at pre-determined time intervals in 180 min, and analyzed for residual $FeCl_3$ ion concentrations. Due to the $FeCl_3$ solutions own gravity, the filtrates were collected only 2.5 mL after 180 min. A small amount of filtrates solution has negligible effect on the concentration of the salt concentration during the adsorption experiments.

The adsorption efficiency (AE) was calculated by using the following expression S(1) :

$$AE=\left(1-\frac{C_a}{C_0}\right)*100\% \qquad S(1)$$

where C_o and C_a (mg L^{-1}) are the initial solution concentrations and final solution concentrations after adsorption equilibrium, respectively.

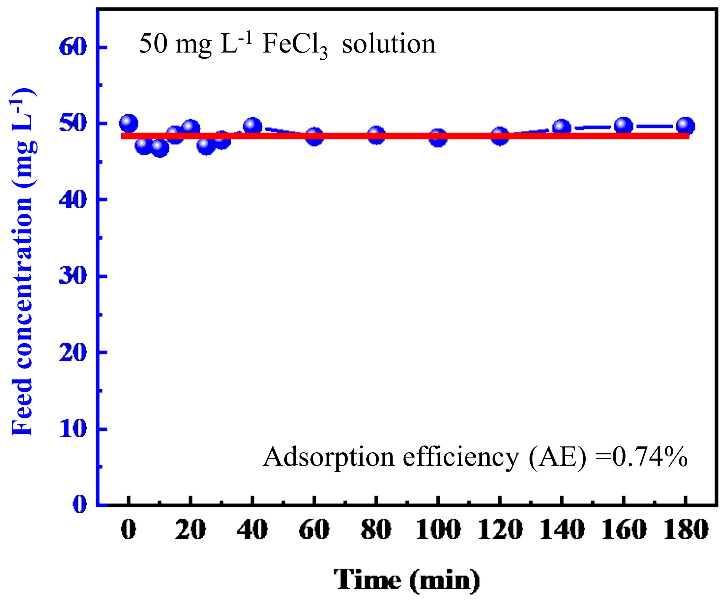

Fig. S9 The adsorption experiment for F-GO membrane in 50 mg L^{-1} $FeCl_3$ solution.

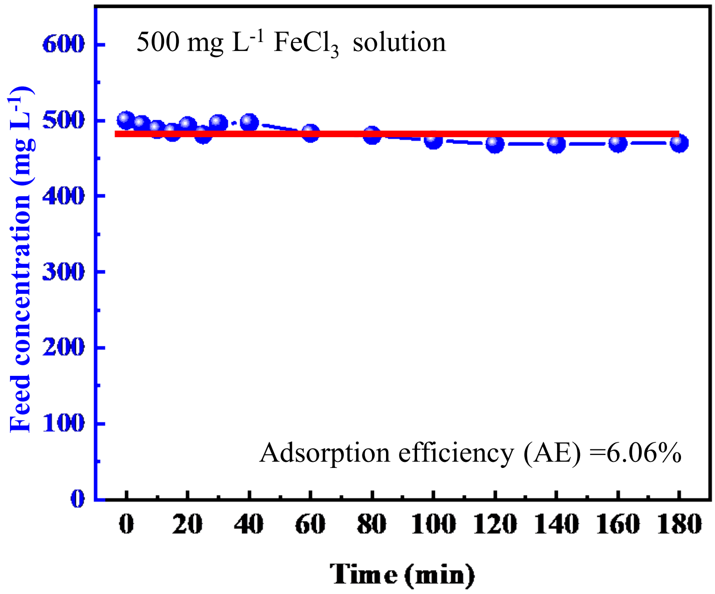

Fig. S10 The adsorption experiment for F-GO membrane in high concentration 500 mg L^{-1} $FeCl_3$ solution.

PS8. Comparisons of water permeance and rejection for high valence ions of F-GO membranes in this work with other NF membranes in literatures.

Table S3. Comparisons of water permeance and rejection for high valence ions of F-GO membranes in this work with other NF membranes in literature.

Membrane	Test condition	Salts or ions	Rejection	Permeance (L h^{-1} m^{-2} bar^{-1})	References
GO-IPDI membrane	0.1 mM ,1bar	$Cr(NO_3)_3$	71.1%	100	S 1
PDA/TFC composite membrane	500 mg L^{-1}, 4 bar	$Pb(NO_3)_2$	91.1%	3.5	S 2
GO/Torlons composite membrane	1000 mg L^{-1}, 3bar	$Pb(NO_3)_2$	95%	4.7	S 3
PSE-GO-DMF	50 mg L^{-1}, 414 kPa	Cr^{3+}	91.2%	13.5	S 4
trGOM	0.1 mM, 2 bar	Cu^{2+}	65.4%	0.27	S 5
HNTs decorated commercial NF membranes	5 mg L^{-1}, 3 bar	Cu^{2+}	74.3%	13.9	S 6
γ-Al_2O_3/α-Al_2O_3 hollow fiber	2000 mg L^{-1}, 5.0 bar	$FeCl_3$	97.1%	17.4	S 7
PDA functionalized nanotube PEI	1000 mg L^{-1}, 3 bar	$Pb(NO_3)_2$	79.0%	50.0	S 8

membranes					
Commercial NF	2000 mg L^{-1}, 6-15bar	$MgSO_4$	40%-98%	5-14	S 9
DK	50 mg L^{-1}, 2bar	$MgSO_4$	56.5%	7.3	S 9
DL	50 mg L^{-1},2bar	$MgSO_4$	60.7%	6.2	S 9
PA-1/MCE	1000 mg L^{-1}, 2bar	$MgSO_4$	98%	60	S10
rGO–K^+	100 mg L^{-1}, 1bar	$FeCl_3$	99.8%	86.1	S11
GO	50 mg L^{-1}, 1 bar	$FeCl_3$	99.9	75	S12
AH-rGO	50 mg L^{-1}, 1bar	$FeCl_3$	91.6%	142.5	S13
hrGO-Trp	50 mg L^{-1}, 1bar	$FeCl_3$	98.2%	191.0	S14
	50 mg L^{-1}, 1bar	$FeCl_3$	99.9%	219.7	
F-GO	50 mg L^{-1}, 1bar	$CrCl_3$	99.7%	198.4	This Work
	50 mg L^{-1}, 1bar	$CuSO_4$	99.4%	199.1	
F-GO (50 nm)	50 mg L^{-1}, 1bar	$FeCl_3$	99.0%	305.0	

PS9. Water permeances and rejection for the F-GO membranes with different anions.

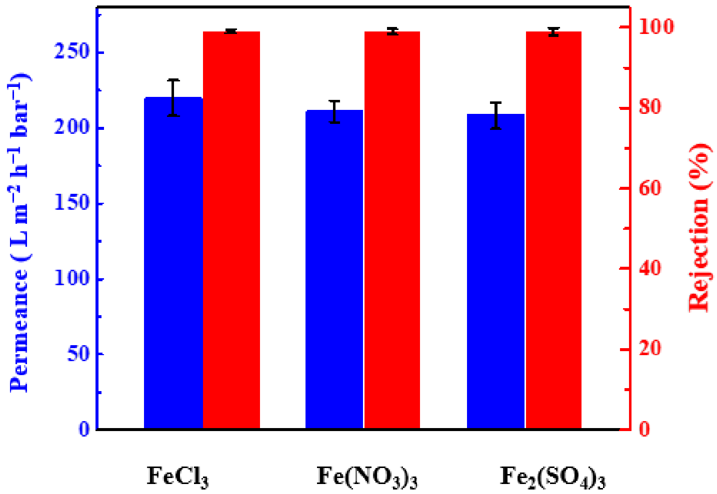

Fig. S11. Water permeances and rejection for the F-GO membranes with different anions.

PS10. The rejections and water permeances of F-GO membrane for different concentrations of $FeCl_3$ solutions.

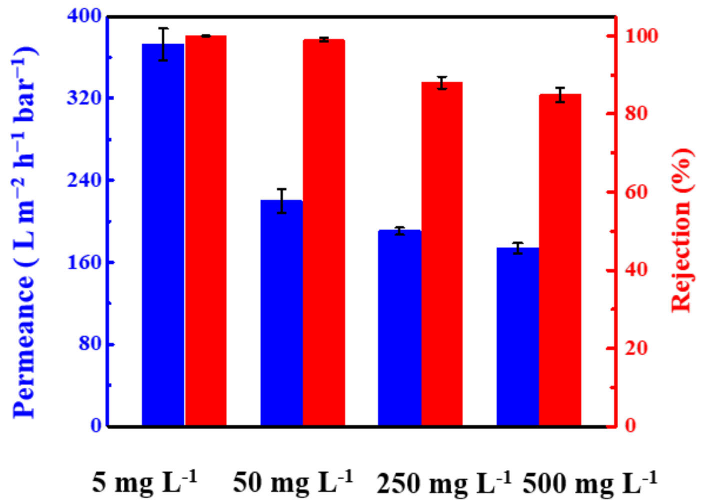

Fig. S12 The rejections and water permeances of F-GO membrane for different concentrations of $FeCl_3$ solutions.

PS11. The long-term cross flow stability of the F-GO membrane.

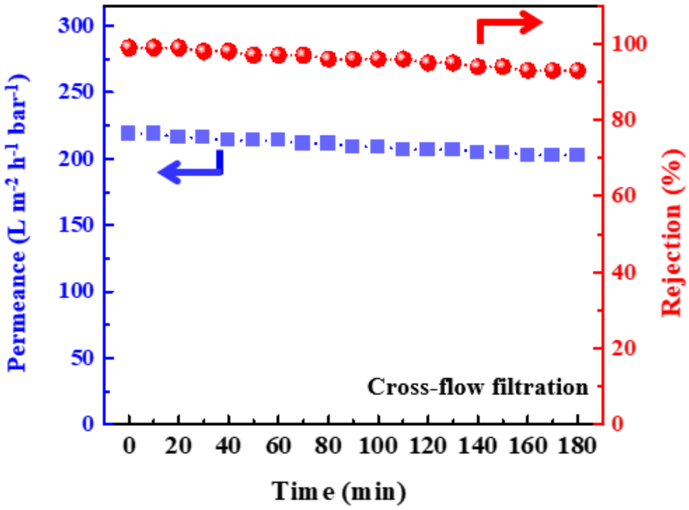

Fig. S13. The long-term cross flow stability of the F-GO membrane for separation of 50 mg L^{-1} $FeCl_3$ solution.

References

S 1 P. Zhang, J.-L. Gong, G.-M. Zeng, C.-H. Deng, H.-C. Yang, H.-Y. Liu and S.-Y. Huan, *Chem. Eng. J.*, 2017, **322**, 657-666.

S 2 T. Wang, H. Qiblawey, E. Sivaniah and A. Mohammadian, *J. Membr. Sci.*, 2016, **511**, 65-75.

S 3 Y. Zhang, S. Zhang, J. Gao and T.-S. Chung, *J. Membr. Sci.*, 2016, **515**, 230-237.

S 4 R. Mukherjee, P. Bhunia and S. De, *Chem. Eng. J.*, 2016, **292**, 284-297.

S 5 J.-H. Jang, J. Y. Woo, J. Lee and C.-S. Han, *Environ. Sci. Technol.*, 2016, **50**, 10024-10030.

S 6 X. Liu, P. Feng, L. Zhang and Y. Chen, *Polym. Adv. Technol.*, 2020, **31**, 665–674.

S 7 *J. Membr. Sci.*, 2016, **503**, 69-80.

S 8 R. S. Hebbar, A. M. Isloor, K. Ananda and A. F. Ismail, *J. Mater. Chem. A*, 2016, **4**, 764-774.

S 9 M. Zhang, K. Guan, Y. Ji, G. Liu, W. Jin and N. Xu, *Nat. Commun.*, 2019, **10**, 1253.

S10 L. Gui, J. Dong, W. Fang, S. Zhang, K. Zhou, Y. Zhu, Y. Zhang and J. Jin, *Nano Lett.*, 2020, **20**, 5821-5829.

S11 R. Yang, Y. Fan, R. Yu, F. Dai, J. Lan, Z. Wang, J. Chen and L. Chen, *J. Membr. Sci.*, 2021, **635**, 119437.

S12 F. Dai, F. Zhou, J. Chen, S. Liang, L. Chen and H. Fang, *J. Mater. Chem. A*, 2021, **9**, 10672-10677.

S13 F. Dai, R. Yu, R. Yi, J. Lan, R. Yang, Z. Wang, J. Chen and L. Chen, *Chem. Commun.*, 2020, **56**, 15068-15071.

S14 J. Liu, S. Wang, R. Yang, L. Li, S. Liang and L. Chen, J. Membr. Sci., 2022, 120745.